Original Article

Exploring Nanoherbal *Paraboea leuserensis* as a Therapeutic Agent in Traumatic Brain Injury: *In Silico*, and *In Vivo* Approaches

Syafruddin Ilyas[1], PhD; Putri Cahaya Situmorang[1], PhD; Hafandi Ahmad[2], PhD; Dina Khairani[1], MSc; Dini Prastyo Wati[1], MSc; Wardah Sawitri Polem[1], MSc

[1]Study Program of Biology, Faculty of Mathematics and Natural Sciences, Universitas Sumatera Utara, Medan, Indonesia;
[2]Department of Veterinary Preclinical Sciences, Faculty of Veterinary Medicine, University of Putra Malaysia, Selangor, Malaysia

Correspondence:
Syafruddin Ilyas, PhD;
Study Program of Biology, Faculty of Mathematics and Natural Sciences, Universitas Sumatera Utara, Postal Code: 20155, Medan, Indonesia
Email: syafruddin6@usu.ac.id
Received: 06 March 2025
Revised: 08 July 2025
Accepted: 08 August 2025

What's Known

- Traumatic brain injury (TBI) is a major health issue with limited therapeutic options.
- Natural compounds with anti-inflammatory and neuroprotective properties have shown potential in TBI treatment.
- Certain bioactive compounds, including fatty acids and silane derivatives, possess pharmacokinetic properties that enable blood-brain barrier penetration and neuroprotection.

What's New

- This study identifies nanoherbal *Paraboea leuserensis* as a novel therapeutic candidate for TBI.
- Molecular docking confirms strong interactions with ERK2, CCR2, and JNK3, suggesting neuroprotective effects.
- *In vivo* tests show increased SOD activity and reduced MDA levels, highlighting its antioxidative and anti-inflammatory potential.
- Findings support its development for neural recovery and pharmaceutical applications.

Abstract

Background: Traumatic brain injury (TBI) is a major global health burden and one of the leading causes of death and disability worldwide, affecting up to 74 million people annually. It profoundly impairs mental health, quality of life, and daily functioning. This study aimed to explore the therapeutic potential of nanoherbal compounds from *Paraboea leuserensis* using combined *in silico* and *in vivo* approaches in a rat model of TBI.

Methods: In the *in silico* phase, bioactive compounds from *Paraboea leuserensis* leaves identified by Gas Chromatography–Mass Spectrometry (GC-MS) were screened through molecular docking to assess their binding affinity and pharmacokinetic properties. For the *in vivo* study, 30 male Wistar rats were allocated into six groups: G0 (normal control), G+(TBI control), MP (TBI+methylprednisolone 30 mg/Kg BW), and treatment groups PL100, PL200, and PL300 (TBI+nanoherbal extract at 100, 200, and 300 mg/Kg BW, respectively). Antioxidant activity was evaluated through superoxide dismutase (SOD) and malondialdehyde (MDA) assays. Data were analyzed by one-way ANOVA with Tukey's post hoc test ($P<0.05$) using GraphPad Prism.

Results: GC-MS analysis revealed bioactive compounds with favorable pharmacokinetic properties. Molecular docking showed strong interactions of 9-octadecen-12-ynoic acid methyl ester with ERK2 and CCR2, while 9-octadecenoic acid (Z) displayed notable binding to JNK3. *In vivo*, PL100 ($P<0.01$), PL200 ($P<0.001$), and PL300 ($P<0.0001$) significantly enhanced SOD activity and reduced MDA levels compared to the TBI control.

Conclusion: Both *in silico* and *in vivo* findings highlight the neuroprotective potential of *Paraboea leuserensis*, with PL300 showing the most pronounced antioxidant effect in TBI-induced rats.

Please cite this article as: Ilyas S, Cahaya Situmorang P, Ahmad H, Khairani D, Prastyo Wati D, Sawitri Polem W. Exploring Nanoherbal *Paraboea leuserensis* as a Therapeutic Agent in Traumatic Brain Injury: *In Silico*, and *In Vivo* Approaches. Iran J Med Sci. doi: 10.30476/ijms.2025.106167.4027.

Keywords ● Traumatic brain injury ● Phytotherapy ● Molecular docking simulation ● Oxidative stress ● Superoxide dismutase

Introduction

Traumatic brain injury (TBI) is a significant global public health issue and is among the leading causes of mortality and disability, affecting an estimated 64–74 million individuals annually.[1] TBI is a common neurological injury with a high morbidity rate. Its impact on mental health is increasingly recognized as a major

consequence, potentially affecting the quality of life and daily functioning.[2] The etiology of TBI includes various factors, such as falls, traffic accidents, sports-related injuries, and physical violence, including blast injuries. The mechanisms of injury are influenced by factors such as geographic region, socioeconomic status, age, and sex.[3] Post-TBI symptoms may encompass physical manifestations, such as nausea, dizziness, and blurred vision, as well as cognitive and emotional disturbances, such as executive dysfunction, depression, and anxiety.[4]

The pathological mechanisms of TBI encompass both primary and secondary damage. Secondary damage, which occurs post-trauma, involves the activation of various cellular signaling pathways, including the inflammatory response. Cellular mechanosensors compromised by high pressure can initiate ongoing injury, particularly in cases of repeated trauma.[5] Following injury, a complex interaction transpires between pro-inflammatory and anti-inflammatory signaling pathways involving extracellular signal-regulated kinase 2 (ERK2), c-Jun N-terminal kinase 3 (JNK3), and C-C chemokine receptor type 2 (CCR2). ERK2 and JNK3 are recognized for their contributions to the production of pro-inflammatory cytokines, thereby exacerbating neuroinflammation, whereas CCR2 is instrumental in recruiting monocytes and microglia to the injury site, further aggravating neuronal damage.[6] Although JNK3 is frequently associated with apoptosis, under certain conditions, it can also promote neuronal survival, indicating a dual role in the pathophysiology of TBI.[7, 8] Consequently, interest in the ERK2, CCR2, and JNK3 signaling pathways in TBI therapy is increasing because of their potential to address inflammation and neurodegeneration. ERK2 and JNK3 regulate inflammatory responses and neuronal apoptosis, whereas CCR2 mediates the recruitment of immune cells, rendering them strategic targets for anti-inflammatory interventions.[9, 10] The administration of corticosteroids, such as methylprednisolone, is a common therapeutic strategy for managing inflammation following TBI. Methylprednisolone acetate, a 6-methyl derivative of prednisolone, is classified as a synthetic glucocorticoid with significant anti-inflammatory effects. This compound is characterized by its appearance as a white crystalline powder, which is insoluble in water but soluble in organic solvents, such as alcohol, chloroform, and methanol. It has a molecular formula of $C_{22}H_{30}O_5$ and a molecular weight of 416.51 Da. Methylprednisolone is extensively used to treat various inflammatory conditions, including multiple myeloma, rheumatic disorders, respiratory diseases, kidney diseases, ocular issues, hematological disorders, neoplastic diseases, nervous system disorders, gastrointestinal illnesses, endocrine dysfunction, and dermatological problems.[11] In the context of TBI, methylprednisolone is employed to suppress secondary inflammatory responses, mitigate cerebral edema, and stabilize cell membranes and pro-inflammatory cytokine production. However, the administration of high doses following TBI may exacerbate apoptosis in the hypothalamic and pituitary regions, potentially leading to critical illness-related corticosteroid insufficiency (CIRCI) and increasing the risk of mortality during the acute phase.[12, 13]

The limitations of methylprednisolone efficacy, coupled with its potential adverse effects, have prompted the pursuit of safer and more natural therapeutic alternatives. Prior research has investigated the application of medicinal plants in the treatment of TBI, with *Aloe vera* and cinnamon emerging as notable candidates due to their demonstrated antioxidant and anti-inflammatory properties, as well as their protective effects on brain tissue in animal models.[14, 15] These findings further substantiate the potential of herbal plants as complementary therapeutic options for managing TBI.

One potential candidate is *Paraboea leuserensis*, an endemic plant from the Leuser ecosystem found in the provinces of Aceh and North Sumatra, including the regions of Dairi, Karo, and Langkat (Indonesia). This plant belongs to the Gesneriaceae family, which comprises approximately 3,500 species from 147–150 genera distributed across tropical and subtropical regions.[16] Among the Karo people, *Paraboea leuserensis* is known as “Gagatan Harimau” and has been traditionally used as a remedy for stomach ailments and as a stamina booster.[17, 18] Pharmacologically, Paraboea is recognized for its anti-inflammatory and antioxidant properties, primarily due to its key bioactive constituents, including flavonoids such as myricetin, myricitrin, quercetin, kaempferol, and ellagic acid. These compounds are widely recognized for their neuroprotective and immunomodulatory effects,[19] making the exploration of *Paraboea leuserensis* as a natural anti-inflammatory agent for TBI therapy highly relevant.

Therefore, this study aimed to evaluate the therapeutic potential of nanoherbal compounds from *Paraboea leuserensis* using *in silico* and *in vivo* approaches in a rat model of TBI. An *in silico* approach is employed to assess the interaction of the compounds with key target proteins involved in post-TBI inflammation and neurodegeneration,

namely ERK2, JNK3, and CCR2, using molecular docking methods. An *in vivo* approach is used to evaluate the biological effects of the compounds on oxidative stress biomarkers, such as MDA levels and SOD activity.

Materials and Methods

Plant Collection and Nanoherbal Preparation

Paraboea leuserensis B.L. Burtt leaves were collected from Timbang Lawan Village, Pancur Batu Subdistrict, Deli Serdang Regency, North Sumatra Province. Plant identification was conducted by the Herbarium Bogoriense BRIN Cibinong (No. B-1216/II.6.2/IR.01.02/6/2023). The collected leaves were then air-dried and ground using a blender. Subsequently, the leaves were processed into nanoparticles using a Planetary Ball Mill (PBM, Changsha Tianchuang Powder Technology Co., Ltd., China) at Nanotech Indonesia.

Gas Chromatography-Mass Spectrometry (GC-MS) Analysis

Bioactive compounds from *Paraboea leuserensis* in 96% ethanol were identified using GC-MS (Shimadzu QP 2010S, Kyoto, Japan), employing Wiley/NIST library software for data analysis. The analysis was conducted with an Rtx-5 ms column measuring 30 m. The injector and detector temperatures were maintained at 250 °C, while the operating temperature ranged from 50 to 300 °C. The column temperature was programmed to increase from 50 °C to 120 °C at a rate of 4 °C per min, held for one min, and then raised from 120 °C to 300 °C at a rate of 6 °C per min, held for 5 min, resulting in a total retention time of 80 min. Helium was used as the carrier gas, with a mass-to-charge ratio range of 50-500 AMU. Electron ionization was performed at 70 eV.[20]

In Silico Experiments

Bioactive Compounds from Paraboea leuserensis : GC-MS analysis (nanoherbal methanol extract) identified seven bioactive compounds from *Paraboea leuserensis* in this study. The identification of these compounds was confirmed using the PubChem database (https://pubchem.ncbi.nlm.nih.gov; National Center for Biotechnology Information, USA) to obtain compound names and their corresponding PubChem CID numbers. The identified compounds included silane (CAS) (PubChem CID: 7918), hexadecanoic acid (CAS) (PubChem CID: 985), 9-Octadecenoic acid (Z) (CAS) (PubChem CID: 445639), and 9-Octadecen-12-ynoic acid methyl ester (CAS) (PubChem CID: 5363161). In addition, three other compounds comprising 3-hydroxymethyl-5-(4-nitroimidazol-l-yl) isoxazole, 3-hexadecyloxycarbonyl-5-(2-hydroxyethyl)-4-methylimidazolium ion, and high-oleic safflower oil (CAS) were also detected, although no corresponding PubChem CID records were available for these compounds.

Drug-Likeness and Pharmacokinetic Prediction: The compounds of the nanoherbal *Paraboea leuserensis* used in this study were obtained from the PubChem database (https://pubchem.ncbi.nlm.nih.gov) in the form of two-dimensional (2D) structures (.sdf format) and Simplified Molecular Input Line Entry System (SMILES) notations. Drug-likeness was evaluated using the SwissADME web server (http://www.swissadme.ch; Swiss Institute of Bioinformatics, Switzerland) based on Lipinski's Rule of Five, which considers molecular weight (≤500 Da), lipophilicity (LogP≤5), hydrogen bond donors (≤5), and hydrogen bond acceptors (≤10) as essential parameters for predicting oral bioavailability.[21] Pharmacokinetic properties, including absorption, distribution, metabolism, and excretion (ADME), were predicted using the pkCSM web server (http://biosig.lab.uq.edu.au/pkcsm/prediction; University of Queensland, Australia). The absorption parameters were assessed based on human intestinal absorption (HIA) and Caco-2 cell permeability, while the distribution properties were evaluated through predictions of blood-brain barrier (BBB) permeability. Metabolism potential was analyzed by determining the interaction of each compound with cytochrome P450 2D6 (CYP2D6), identifying whether the compound acts as a substrate or inhibitor. The excretion potential was assessed using the substrate affinity for organic cation transporter 2 (OCT2). Additionally, aqueous solubility (LogS) was predicted using the Estimated Solubility (ESOL) model to estimate the water solubility of the compounds. The Brain or Intestinal Estimated Permeation Methods (BOILED-Egg model) was also applied to visualize the probability of HIA and BBB permeability, providing a comprehensive prediction of the pharmacokinetic behavior of these nanoherbal compounds.

Screening of the Biological Activities of Compounds Using the Prediction of Activity Spectra for Substances (PASS) Online Test: The biological activities of compounds derived from the *Paraboea leuserensis* nanoherbal extract were predicted utilizing the Prediction of Activity Spectra of Substances (PASS) online tool, accessible via the Way2drug webserver (http://way2drug.com/PassOnline/; Institute of Biomedical Chemistry, Russia). Initially, the compound names were entered into the

PubChem database (http://pubchem.ncbi.nlm.nih.gov) to retrieve the corresponding SMILES structures. These SMILES were subsequently uploaded to the PASS server to predict the potential biological activities. PASS analysis yielded two critical parameters for each compound: Pa (probability of activity) and Pi (probability of inactivity). A compound is deemed to possess potential biological activity when its Pa value surpasses its Pi value. According to the PASS prediction criteria, the Pa is categorized into three levels: Pa>0.7 indicates a high likelihood of biological activity, 0.5<Pa<0.7 suggests moderate activity, and Pa<0.5 indicates a low probability of activity.[22, 23]

Molecular Docking

Molecular docking was executed using BIOVIA Discovery Studio software (BIOVIA, Dassault Systèmes, France) for ligand preparation, where ligand structures were initially downloaded from the PubChem database (http://pubchem.ncbi.nlm.nih.gov) and saved in SDF format for further analysis. The ligands underwent energy minimization utilizing Open Babel software integrated with PyRx v.0.8 (The Scripps Research Institute, USA), which included not only the phytochemical compounds from *Paraboea leuserensis* but also native ligands and appropriate standard drugs.[23] The three-dimensional structures of the target proteins ERK2 (PDB ID: 5NHJ), CCR2 (PDB ID: 6GPS), and JNK3 (PDB ID: 7KSK) were obtained from the Protein Data Bank (PDB; https://www.rcsb.org/; Research Collaboratory for Structural Bioinformatics, USA) and validated using X-ray diffraction methods, with water molecules removed from the protein structures via PYMOL software (Schrödinger, LLC, USA). Molecular docking and visualization were performed using AutoDock Vina integrated within PyRx v0.8, employing a targeted docking approach with an exhaustiveness setting of 8 to predict the optimal binding poses of the protein-ligand complexes. The grid box parameters (center coordinates in X, Y, Z and box dimensions in Å) were defined as follows: ERK2 (center: –6.6501, 8.7536, 33.8196; size: 56.2779×46.5995×92.6204 Å), CCR2 (center: 5.4914, –7.2525, –14.7086; size: 36.0682×26.1593×39.3003 Å), and JNK3 (center: 8.8896, 8.7637, 13.7096; size: 43.9146×38.8612×43.7974 Å).

In Vivo Treatment

Experimental Animals: This study utilized 30 male Wistar rats (200–250 g, 10–15 weeks old) sourced from the Biology Laboratory of Universitas Sumatera Utara (USU), Medan, Indonesia. The rats underwent a two-week acclimatization period in the Animal Physiology Laboratory, Biology Study Program, USU, under controlled conditions (12-hour light/dark cycle, 35–60% humidity) in plastic cages (40×30 cm) sterilized by radiation. The animals were provided *ad libitum* access to water, corn, and standard pellets. The study was approved by the Health Research Ethics Committee of USU Medan (No. 01019/KEPH-FMIPA/2023). The rats were randomly assigned to six groups (n=5/group): G0 (negative control), G+ (subjected to TBI induced by a 50 g weight drop from a height of 2 m), MP (TBI+methylprednisolone 10 mg/Kg BW), PL100 (TBI+nanoherbal *Paraboea leuserensis* 100 mg/Kg BW), PL200 (TBI+nanoherbal *Paraboea leuserensis* 200 mg/Kg B), and PL300 (TBI+nanoherbal *Paraboea leuserensis* 300 mg/Kg BW). The test drugs and compounds were administered orally once daily for 30 consecutive days.

SOD and MDA Analysis: At the end of the experimental period, the rats were euthanized by intramuscular injection of a lethal dose of euthanasia solution into the thigh muscle, a method that may require a slightly longer onset compared to intravenous administration. Following euthanasia, blood samples were collected via cardiac puncture, allowed to clot at room temperature, and centrifuged at 3000 rpm for 15 min to obtain serum for biochemical analyses. The levels of SOD and MDA were measured using commercial ELISA kits (Sigma-Aldrich, USA) according to the manufacturer's protocols to assess antioxidant capacity and lipid peroxidation, respectively.

Statistical Analysis

Data are expressed as mean±SEM. Statistical analyses were conducted using one-way ANOVA, followed by Tukey's *post-hoc* test, using GraphPad Prism version 10.0.0 (GraphPad Software Inc., San Diego, CA, USA). Statistical significance was determined at p-values of P<0.05 (*), P<0.01 (**), P<0.001 (***), and P<0.0001 (****).

Results

GC-MS Analysis

The results of the GC-MS analysis showed the presence of several compounds with varying retention times and concentrations, as shown in table 1, along with the chromatogram in figure 1. The compounds detected included silane (CAS) with a percentage of 24.94%, hexadecanoic acid (CAS) at 26.49%, 9-octadecenoic acid (Z) at 37.54%, 9-octadecene-12-ynoic acid, methyl ester 1.73%, and hi-oleic sunflower oil 0.98%.

Table 1: Identified compounds of the nanoherbal *Paraboea leuserensis*

No	Compounds name	Molecular formula	Molecular weight	Retention Time (min)	Concentration (%)	Smiles	PubChem ID
1	3-Hydroxymethyl-5-(4-nitroimidazol-l-yl) isoxazolidine	-	-	1.680	7.891	-	-
2	Silane (CAS)	$C_4H_6O_3$	102.09	3.066	24.943	CC(=O)OC(=O)C	7918
3	3-Hexadecyloxycarbonyl-5-(2-hydroxyethyl)-4-methylimidazolium ion	-	-	25.928	0.466	-	-
4	Hexadecanoic acid (CAS)	$C_{16}H_{32}O_2$	256.42	32.744	26.488	CCCCCCCCCCCCCCCC(=O)O	985
5	9-Octadecenoic (Z)-	$C_{18}H_{34}O_2$	282.5	38.003	37.541	CCCCCCCC/C=C\CCCCCCCC(=O)O	445639
6	9-Octadecen-12-ynoic acid, methyl ester (CAS)	$C_{19}H_{32}O_2$	278.4	51.135	1.732	CCCCCC#CC/C=C/CCCCCCCC(=O)OC	5363161
7	Hi-oleic safflower oil (CAS)	-	-	53.415	0.979	-	-

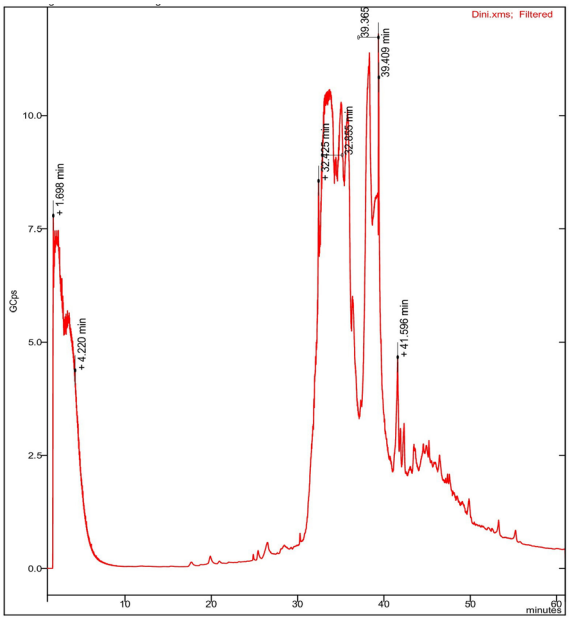

Figure 1: This figure shows the Gas Chromatography–Mass Spectrometry (GC-MS) chromatogram of the nanoherbal *Paraboea leuserensis*.

Drug-Likeness Prediction and Pharmacokinetics Prediction

Based on the analysis using Lipinski's rule, several compounds evaluated in this study demonstrate potential for use as drugs despite violations of specific parameters. The results are summarized in table 2. Silane (CAS) does not violate Lipinski's rule, indicating potential for oral bioavailability. The physicochemical properties of this compound align with characteristics typically associated with compounds easily absorbed by the body. Hexadecanoic acid (palmitic acid) exhibits high lipophilicity, which can affect its water solubility and may reduce oral bioavailability. However, palmitic acid is still commonly used in pharmaceutical formulations, particularly topical and cosmetic preparations. Additionally, 9-octadecenoic acid (Z)- or oleic acid is widely used in drug formulations, even though its logP value exceeds Lipinski's threshold. Lastly, 9-octadecen-12-ynoic acid, methyl ester (CAS), also demonstrates high lipophilicity.The results of the pharmacokinetic evaluation of *Paraboea leuserensis* nanoherbal compounds, shown in table 2, indicate that all compounds have high HIA values, ranging from 91.82% to 100%. Silane had the highest absorption value (100%) with very acceptable solubility and a Caco-2 permeability of 1.18, indicating a high ability to pass through the intestinal membrane. Hexadecanoic acid has an absorption value of 92%, Caco-2 permeability of 1.1558, and is moderately soluble. The compound 9-octadecen-12-ynoic acid methyl ester showed an absorption value of 93.63%, the highest Caco-2 permeability of 1.583, and moderate solubility, indicating very acceptable potential for membrane absorption and transport. Meanwhile, 9-octadecenoic acid had the lowest absorption value of 91.82% but remained high, with a Caco-2 permeability of 1.563 and moderate solubility. None of these compounds acted as CYP2D6 inhibitors or OCT2

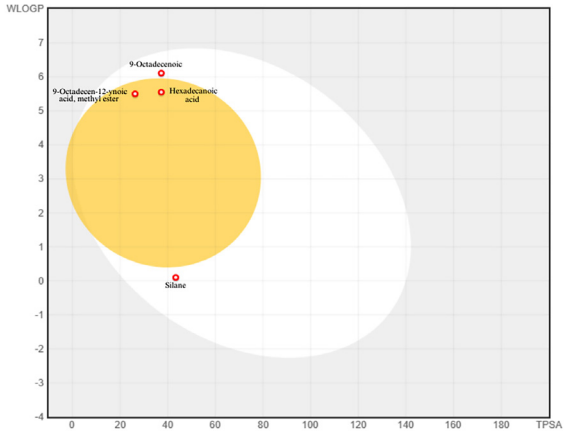

Figure 2: This figure shows the prediction of brain and intestinal permeability of the nanoherbal *Paraboea leuserensis* components using the BOILED-Egg predictive model, where white indicates Human Intestinal Absorption (HIA) and yellow indicates the Blood-Brain Barrier (BBB).

Table 2: Lipinski's rule of five assessment and pharmacokinetic profile predictions for compounds from nanoherbal *Paraboea leuserensis*

No	Compound name	Lipinski				Violation	Pharmacokinetic characteristics						
		MW	MlogP ≤4.15	NorO ≤10	NHorOH ≤5		Human Intestinal Absorption	Caco-2 permeability	BBB permeability	CYP2D6 substrate	CYP2D6 inhibitor	OCT2 substrate	LogS (ESOL)
1	Silane (CAS)	102.09	0.31	0	3	0	100%	1.18	-0.281 (No)	No	No	No	Very soluble
2	Hexadecanoic acid (CAS)	256.42	4.19	1	2	1	92%	1.1558	-0.111 (Yes)	No	No	No	Moderately soluble
3	9-Octadecenoic (Z)-	282.5	4.57	1	2	1	91.82%	1.563	-0.168 (No)	No	No	No	Moderately soluble
4	9-Octadecen-12-ynoic acid, methyl ester (CAS)	278.4	4.47	1	2	1	93.63%	1.583	-0.09 (Yes)	No	No	No	Moderately soluble

MW: Molecular weight; MlogP: Moriguchi logarithm of partition coefficient; NorO: Number of nitrogen; NHorOH: Number of NH or OH; Caco-2 permeability: Caco-2 cell monolayer permeability; BBB permeability: Blood-brain barrier permeability; CYP2D6: Cytochrome P450 2D6; OCT2 substrate: Organic cation transporter 2 substrate; LogS: Logarithm of solubility

Table 3: Prediction of the biological activity of nanoherbal *Paraboea leuserensis*

No	Compound name	Biological activity	Pa	Pi	Criteria
1	Silane (CAS)	Anti-inflammatory	0.550	0.043	High
		Neuropathy treatment	0.630	0.010	High
		Antineurotic	0.529	0.098	High
		Antioxidant	0.183	0.067	Low
		Apoptosis agonist	0.309	0.122	Low
		GABA C receptor agonist	0.657	0.004	High
2	Hexadecanoic acid (CAS)	GABA aminotransferase inhibitor	0.852	0.002	Very high
		Anti-inflammatory	0.515	0.052	High
		Antioxidant	0.222	0.045	Low
		Neurotransmitter antagonist	0.624	0.009	High
		Antineurogenic pain	0.271	0.095	Low
		Antineurotic	0.555	0.088	High
		GABA C receptor agonist	0.686	0.004	High
		Apoptosis antagonist	0.417	0.006	Low
3	9-Octadecenoic (Z)-	GABA aminotransferase inhibitor	0.820	0.003	Very high
		GABA C receptor antagonist	0.256	0.025	Low
		GABA C receptor agonist	0.659	0.004	High
		Anti-inflammatory	0.614	0.029	High
		Neurotransmitter antagonist	0.547	0.025	High
		Antineurogenic pain	0.253	0.120	Low
		Apoptosis antagonist	0.471	0.004	Low
		Apoptosis agonist	0.499	0.040	Low
4	9-Octadecen-12-ynoic acid, methyl ester (CAS)	GABA C receptor agonist	0.498	0.011	Low
		GABA C receptor antagonist	0.298	0.015	Low
		GABA aminotransferase inhibitor	0.750	0.004	Very high
		Neurotransmitter antagonist	0.481	0.048	Low
		Antiinflammatory	0.559	0.041	High
		Apoptosis antagonist	0.346	0.014	Low

Pa: Probability activity; Pi: Probability inactivity

substrates, indicating a stable renal metabolism and elimination profile and minimal risk of drug interactions. Based on the prediction of compound distribution using the BOILED-Egg model shown in figure 2, silane and 9-octadecenoic acid are in the white area, indicating proper intestinal absorption but are unable to penetrate the BBB. In contrast, hexadecanoic acid and 9-octadecen-12-ynoic acid methyl ester are located in the yellow area, indicating their ability to cross the BBB and potentially reach the central nervous system (CNS). Based on the pharmacokinetic parameters in table 2 and the predictive distribution in figure 2, hexadecanoic acid and 9-octadecen-12-ynoic acid methyl ester were considered the best candidates because they had the best absorption profile, permeability, and BBB penetration ability.

Bioactivity Prediction of the Nanoherbal Paraboea leuserensis Compounds by PASS Online Test

According to the PASS Online prediction, Pa values approaching 1 suggest a higher likelihood of biological activity, with values exceeding 0.7 classified as very high, those between 0.5 and 0.7 as high, and those below 0.5 as low. As shown in table 3, hexadecanoic acid exhibited the most favorable bioactivity profile relevant to TBI, showing potential as a GABA aminotransferase inhibitor (Pa 0.852), GABA C receptor agonist (Pa 0.686), anti-inflammatory agent (Pa 0.515), and antineurotic agent (Pa 0.555). These predicted activities suggest that hexadecanoic acid may enhance GABAergic neurotransmission and reduce neuroinflammation, thus highlighting its potential as a promising candidate for TBI therapy.

Molecular Interactions of Nanoherbal Paraboea leuserensis Compounds with ERK2, CCR2, and JNK3

In this study, molecular docking simulations were performed to examine the interactions of nanoherbal compounds derived from *Paraboea leuserensis* with three target proteins: ERK2 (5NHJ), CCR2 (6GPS), and JNK3 (7KSK). The results of the docking, detailed in table 4 and table 5, and illustrated in figure 3, reveal significant differences in interaction types and binding energies among the tested compounds.

Table 4: Binding energy of the nanoherbal *Paraboea leuserensis* compound

No	Compounds name	Biding Energy		
		ERK2 (5NHJ)	CCR2 (6GPS)	JNK3 (7KSK)
1	Control positive (Methylprednisolone)	-7.2	-7.7	-7.5
2	Silane (CAS)	-4.6	-4.7	-3.8
3	Hexadecanoic acid (CAS)	-5.2	-5.9	-5.5
4	9-Octadecenoic (Z)-	-6.1	-6.8	-6.1
5	9-Octadecen-12-ynoic acid, methyl ester (CAS)	-6.2	-6.2	-5.7

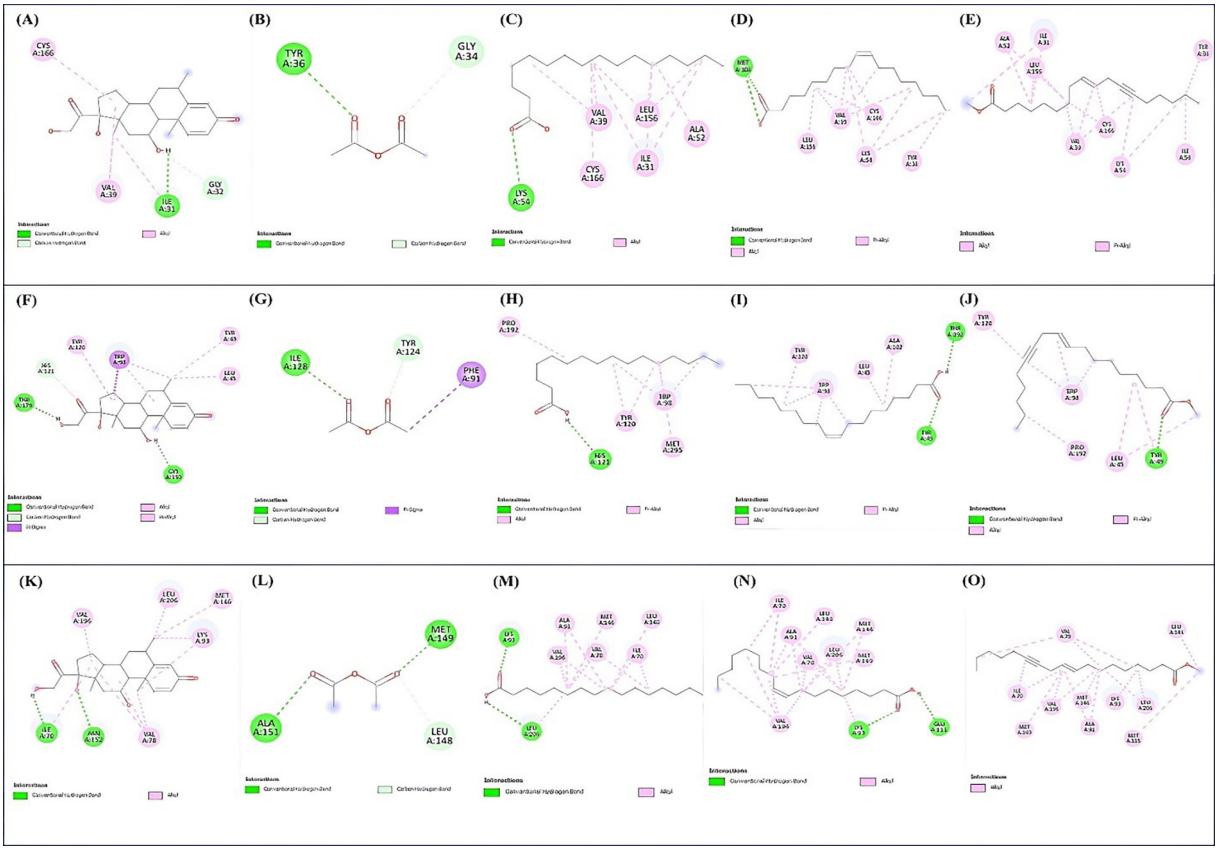

Figure 3: 2D visualization of ligand–protein interactions of ERK2, CCR2, and JNK3 with various ligands: (A) ERK2 with positive control methylprednisolone, (B) ERK2 with silane, (C) ERK2 with hexadecanoic acid and phenyl salicylate, (D) ERK2 with 9-octadecenoic acid, (E) ERK2 with 9-octadecen-12-ynoic acid methyl ester, (F) CCR2 with positive control methylprednisolone, (G) CCR2 with silane, (H) CCR2 with hexadecanoic acid and phenyl salicylate, (I) CCR2 with 9-octadecenoic acid, (J) CCR2 with 9-octadecen-12-ynoic acid methyl ester, (K) JNK3 with positive control methylprednisolone, (L) JNK3 with silane, (M) JNK3 with hexadecanoic acid and phenyl salicylate, (N) JNK3 with 9-octadecenoic acid, and (O) JNK3 with 9-octadecen-12-ynoic acid methyl ester.

Table 5: Residues of ligands/compounds from nanoherbal *Paraboea leuserensis* with ERK2, CCR2, and JNK3 interaction

No	Ligand	Interaction with ERK2			Interaction with CCR2			Interaction with JNK3		
		Conventional hydrogen bond	Carbon hydrogen	Hydrophobic	Conventional hydrogen bond	Carbon hydrogen	Hydrophobic	Conventional hydrogen bond	Carbon hydrogen	Hydrophobic
1	Methylprednisolone	A:ILE31	A:GLY32	A:VAL39 A:CYS166	A:THR179 A:CYS190	A:HIS121	A:LEU45 A:TYR49 A:TRP98 A:TYR120	A:ILE70 A:ASN152		A:VAL78 A:LYS93 A:MET146 A:VAL196 A:LEU206
2	Silane (CAS)	A:TYR36	A:GYL34	-	A:ILE128	A:TYR124	A:PHE91	A:MET149 A:ALA151	A:LEU148	-
3	Hexadecanoic acid (CAS)	A:LYS54		A:ILE31 A:VAL39 A:ALA52 A:LEY156 A:CYS166	A:HIS121		A:TRP98 A:TYR120 A:PRO192 A:MET295	A:LYS93 A:LEU206		A:ILE70 A:VAL78 A:ALA91 A:MET146 A:LEU148 A:VAL196
4	9-Octadecenoic (Z)-	A:MET108		A:TYR36 A:VAL39 A:LYS54 A:LEU156 A:CYS166	A:TYR49 A:THR292	A:LEU45 A:TRP98 A:ALA102 A:TYR120		A:LYS93 A:GLU111		A:ILE70 A:VAL78 A:ALA91 A:MET146 A:LEU148 A:MET149 A:VAL196 A:LEU206
5	9-Octadecen-12-ynoic acid, methyl ester (CAS)			A:ILE31 A:TYR36 A:VAL39 A:ALA52 A:LYS54 A:ILE56 A:LEU156 A:CYS166	A:TYR49	A:LEU45 A:TRP98 A:TYR120 A:PRO192				A:ILE70 A:VAL78 A:ALA91 A:LYS93 A:MET115 A:LEU144 A:MET146 A:MET149 A:VAL196 A:LEU206

The positive control, methylprednisolone, displayed the most potent binding energies, measuring -7.2 kcal/mol for ERK2, -7.7 kcal/mol for CCR2, and -7.5 kcal/mol for JNK3, with notable hydrogen bonds and hydrophobic interactions occurring with key residues such as ILE31, GLY32, and CYS166 on ERK2, as well as THR179, CYS190, and HIS121 on CCR2. Among the four compounds analyzed from *Paraboea leuserensis*, 9-octadecen-12-ynoic acid, methyl ester exhibited the best binding energies, closely rivaling those of methylprednisolone at -6.2 kcal/mol for both ERK2 and CCR2 and showing significant interactions with ILE31 and TYR36 on ERK2, as well as TYR49 and LEU45 on CCR2, indicating promising biological potential. For JNK3, 9-octadecenoic (Z)-acid had the best binding energy at -6.1 kcal/mol, with critical interactions involving LYS93 and GLU111, while hexadecanoic acid displayed a lower binding energy of -5.5 kcal/mol for JNK3, interacting with LYS93 and LEU206, which suggests a lower affinity than 9-octadecenoic (Z)-acid.

In Vivo SOD and MDA Assay

The results of the examinations of MDA and SOD in rat blood serum after the administration of *Paraboea leuserensis* are illustrated in figure 4. The data revealed an increased activity of SOD following treatment with the nanoherbal compound, indicating its potential antioxidant protection against cellular damage caused by free radicals. Additionally, a decrease in MDA levels was observed, suggesting the neuroprotective properties of the nanoherbal compound, which may enhance the activity of the body's antioxidant system.

Discussion

This study elucidates the potential of nanoherbal *Paraboea leuserensis* leaf as a therapeutic candidate for TBI through an integrated approach that includes GC-MS analysis, pharmacokinetic and drug-likeness predictions, molecular docking simulations, and *in vivo* testing. The GC-MS analysis identified several

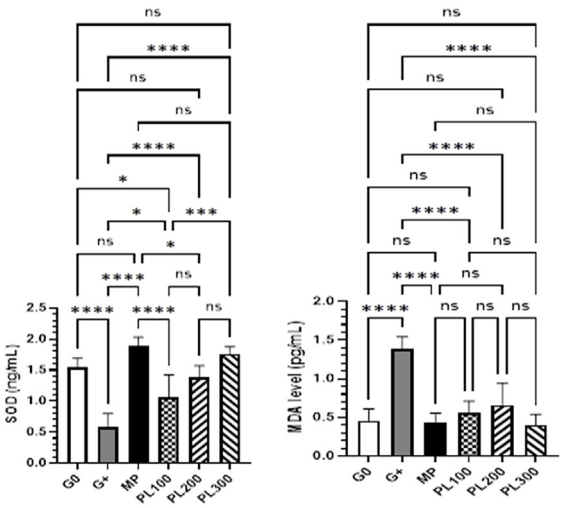

Figure 4: Values of SOD and MDA levels of rat blood serum administered with nanoherbal *Paraboea leuserensis*. The data are expressed as the average levels of MDA and SOD in serum (n=5). Signs *P<0.05, **P<0.01, ***P<0.001, and ****P<0.0001. G0: negative control; G+: TBI 50 g with a height of 2 m (TBI 50 g), MP: TBI 50 g+methylprednisolone 10 mg/Kg BB; PL100: TBI 50 g+100 mg/Kg BW; PL200: TBI 50 g+200 mg/Kg BW; PL300: TBI 50 g+300 mg/Kg BW.

bioactive compounds that may contribute to neuroprotection in TBI. Silane (CAS), although primarily utilized in industrial applications,[24] may enhance the stability and delivery efficiency of active compounds when incorporated into nanoparticle systems. Hexadecanoic acid (palmitic acid), detected in high concentration, has been reported to exhibit anti-inflammatory activity,[25] which is crucial for modulating the excessive inflammatory response following TBI. Furthermore, the identification of 9-octadecenoic acid (Z), a monounsaturated fatty acid with known antioxidant and cardioprotective properties,[26] suggests its role in reducing oxidative stress in brain tissue, which is an important factor in secondary neuronal damage following injury. The methyl ester of 9-octadecenoic-12-ynoic acid, despite limited pharmacological data, may offer unique chemical reactivity that supports tissue repair. The presence of hi-oleic safflower oil indicates potential neuroprotective benefits through lipid metabolism modulation and cholesterol regulation.[27] Overall, this bioactive compound profile supports the hypothesis that nanoherbal *Paraboea leuserensis* may reduce oxidative stress and inflammation, thereby serving as a promising adjunctive therapeutic agent for TBI management.

In this study, the assessment of Lipinski's rule indicated that several nanoherbal compounds derived from *Paraboea leuserensis* leaves hold potential as drug candidates, despite certain parameter violations. Silane (CAS) fully complies with Lipinski's drug-likeness criteria, suggesting favorable oral bioavailability. However, its primary application lies in material science rather than therapeutic contexts, necessitating further exploration of its pharmacological potential.[28] Additionally, hexadecanoic acid, 9-octadecenoic acid (Z), and 9-octadecen-12-ynoic acid methyl ester violate one Lipinski parameter related to high lipophilicity. However, they remain promising for use in lipid-based or nanoparticle pharmaceutical formulations to enhance the absorption of active ingredients, either as excipients, lipid delivery systems, or nanoparticle carriers.[26, 29, 30] Subsequent pharmacokinetic analysis revealed that all these compounds exhibited high HIA values and sufficient Caco-2 permeability, supporting their potential for effective oral absorption.[31] Moreover, only hexadecanoic acid and 9-octadecen-12-ynoic acid methyl ester were identified as CYP2D6 substrates without the potential to act as CYP2D6 inhibitors or OCT2 substrates, indicating a low risk of drug–drug interactions via hepatic metabolism and renal elimination pathways.[32, 33] Predictions using the BOILED-Egg model, which estimates a molecule's ability to traverse physiological barriers, further underscore this as a critical pharmacokinetic parameter for drug candidates.[34] These findings reinforce the hypothesis that hexadecanoic acid and 9-octadecen-12-ynoic acid methyl ester from nanoherbal *Paraboea leuserensis* are the most promising bioactive candidates for further development in TBI therapy.

Bioactivity predictions based on PASS Online indicated that several compounds possess significant potential in modulating the GABA system, displaying anti-inflammatory effects and applicability in neuropathy treatment relevant to TBI. The high activity of these compounds, such as GABA C receptor agonists and GABA aminotransferase inhibitors, may contribute to increased GABA levels in the brain, essential for reducing neuronal excitability following TBI.[35] Furthermore, their anti-inflammatory solid activity may mitigate excessive inflammatory responses post-injury, promoting neurological and cognitive recovery by protecting neurons from oxidative stress.[36, 37] While these compounds show promise as therapeutic agents for TBI through GABA modulation and inflammation suppression, their limitations in antioxidant activity and apoptosis modulation necessitate further investigation to optimize their clinical applications. Exploring these compounds in clinical trials and animal models related to TBI is crucial to confirm their therapeutic effectiveness.

In this study, molecular docking simulations

were conducted to explore the interactions of nanoherbal compounds derived from *Paraboea leuserensis* with three critical target proteins: ERK2 (5NHJ), CCR2 (6GPS), and JNK3 (7KSK). These proteins are critical in cellular pathways related to inflammatory responses and stress, particularly in TBI, where intricate cellular mechanisms are activated. The role of ERK2 is particularly noteworthy, as it regulates neuronal survival and synaptic plasticity, exhibiting effects that can be neuroprotective or neurotoxic depending on the microenvironment.[9] CCR2 facilitates the recruitment of immune cells to the injury site, enhancing necessary inflammatory processes for recovery.[38] In contrast, JNK3, a neuron-specific kinase, contributes to neurodegeneration following TBI through the phosphorylation of c-Jun in response to stress.[7, 8]

The TBI model employed in this study was induced *in vivo* by dropping a 50 g weight from a height of 2 m, effectively resulting in closed traumatic brain injury in rats. This methodology facilitated the assessment of oxidative stress biomarkers, specifically SOD and MDA, in the context of secondary brain injury. The observed significant increase in SOD activity within the treatment groups underscores the antioxidant protective potential of nanoherbal *Paraboea leuserensis* in mitigating oxidative stress induced by free radicals. These findings imply that one of the neuroprotective mechanisms of this nanoherbal formulation is its capacity to regulate oxidative stress and enhance the antioxidant defense system following TBI. Elevated SOD activity is instrumental in scavenging superoxide radicals, thereby reducing cellular damage and preserving neurons' integrity. Conversely, the reduction in MDA levels post-treatment further corroborates the antioxidant activity of *Paraboea leuserensis*, as MDA serves as a marker of lipid peroxidation, and its decrease indicates diminished oxidative damage.[39, 40] Collectively, these *in vivo* results substantiate the potential of *Paraboea leuserensis* as a therapeutic agent for reducing oxidative stress and supporting neuronal protection in post-TBI conditions.

These findings collectively highlight the potential of *Paraboea leuserensis* in providing antioxidant properties or augmenting the body's intrinsic antioxidant defenses, which is particularly significant in TBI recovery contexts. Such characteristics open avenues for developing innovative therapies to reduce the adverse effects of brain injuries. The interactions observed through molecular docking simulations and the promising biochemical outcomes support the hypothesis that nanoherbal compounds from *Paraboea leuserensis* could play a pivotal role in neuroprotection and recovery following TBI.

This study has certain limitations. The *in vivo* evaluation was performed on a single animal model with a limited sample size, which may restrict the extrapolation of results to other biological systems, including humans. Furthermore, although the *in silico* pharmacokinetic and toxicity predictions provided valuable preliminary insights, these findings require further validation through comprehensive biochemical and molecular investigations. In addition, the present study did not assess long-term exposure or potential chronic toxicity of the nanoherbal formulation, leaving its prolonged safety profile uncertain. Future studies incorporating larger sample sizes, multiple animal models, extended observation periods, and detailed mechanistic analyses are warranted to strengthen and expand the current findings.

Conclusion

This study demonstrated the potential of nanoherbal *Paraboea leuserensis* leaves as a therapeutic candidate for TBI using both *in silico* and *in vivo* approaches. Molecular docking analysis revealed that 9-octadecen-12-ynoic acid, methyl ester, exhibited the highest binding affinity toward ERK2 and CCR2 (−6.2 kcal/mol), while 9-octadecenoic acid (Z) showed the strongest interaction with JNK3 (−6.1 kcal/mol). The three main compounds, hexadecanoic acid, 9-octadecenoic acid (Z), and 9-octadecen-12-ynoic acid, methyl ester, also demonstrated favorable pharmacokinetic and ADME profiles, including HIA, Caco-2 permeability, and BBB penetration. These findings were further supported by *in vivo* results, where a dose of PL300 (300 mg/kg BW) was the most effective in enhancing SOD activity and reducing MDA levels, confirming the potential of nanoherbal *Paraboea leuserensi* leaves as a natural neuroprotective agent for TBI therapy. To further support the development of *Paraboea leuserensis* as a therapeutic agent, future research should focus on isolating the most active constituents, optimizing dosage regimens, conducting long-term safety evaluations, and validating efficacy through preclinical and clinical studies.

Acknowledgment

The authors would like to express their gratitude to the General Person in Charge of the 2023 Higher Education Endowment Fund Program (DAPT) for their support and contributions to this research. This research was funded by the 2023 Higher Education Endowment Fund

Program (DAPT) under the Contract for the Implementation of the Equity Project Program for Research and the Formation/Development of Scientific Clusters, and the Center of Excellence for Science and Technology of the Universitas Sumatera Utara for the 2023 Fiscal Year, Number 09/UN5.2.3.1/PPM/KPEP/2023.

Authors' Contribution

S.I: Conceptualization, methodology, supervision, and final review and editing of the manuscript; P.C.S: Data curation, formal analysis, investigation, and drafting of the original manuscript; H.A: Software, validation, visualization, and review and editing of the manuscript; D.K: Supported the investigation, resource provision, project administration, and drafting of the original manuscript; D.P.W: Methodology, validation, formal analysis, and manuscript review and editing; W.S.P: data curation, investigation, resource provision, and manuscript review and editing. All authors have read and approved the final manuscript and agree to be accountable for all aspects of the work in ensuring that questions related to the accuracy or integrity of any part of the work are appropriately investigated and resolved.

Conflict of Interest: None declared.

References

1 Dewan MC, Rattani A, Gupta S, Baticulon RE, Hung YC, Punchak M, et al. Estimating the global incidence of traumatic brain injury. J Neurosurg. 2019;130:1080-97. doi: 10.3171/2017.10.JNS17352. PubMed PMID: 29701556.

2 Howlett JR, Nelson LD, Stein MB. Mental Health Consequences of Traumatic Brain Injury. Biol Psychiatry. 2022;91:413-20. doi: 10.1016/j.biopsych.2021.09.024. PubMed PMID: 34893317; PubMed Central PMCID: PMCPMC8849136.

3 Injury GBDTB, Spinal Cord Injury C. Global, regional, and national burden of traumatic brain injury and spinal cord injury, 1990-2016: a systematic analysis for the Global Burden of Disease Study 2016. Lancet Neurol. 2019;18:56-87. doi: 10.1016/S1474-4422(18)30415-0. PubMed PMID: 30497965; PubMed Central PMCID: PMCPMC6291456.

4 Polinder S, Cnossen MC, Real RGL, Covic A, Gorbunova A, Voormolen DC, et al. A Multidimensional Approach to Post-concussion Symptoms in Mild Traumatic Brain Injury. Front Neurol. 2018;9:1113. doi: 10.3389/fneur.2018.01113. PubMed PMID: 30619066; PubMed Central PMCID: PMCPMC6306025.

5 Keating CE, Cullen DK. Mechanosensation in traumatic brain injury. Neurobiol Dis. 2021;148:105210. doi: 10.1016/j.nbd.2020.105210. PubMed PMID: 33259894; PubMed Central PMCID: PMCPMC7847277.

6 Morganti JM, Riparip LK, Chou A, Liu S, Gupta N, Rosi S. Age exacerbates the CCR2/5-mediated neuroinflammatory response to traumatic brain injury. J Neuroinflammation. 2016;13:80. doi: 10.1186/s12974-016-0547-1. PubMed PMID: 27090212; PubMed Central PMCID: PMCPMC4835854.

7 Wu Y, Zhao Y, Guan Z, Esmaeili S, Xiao Z, Kuriakose D. JNK3 inhibitors as promising pharmaceuticals with neuroprotective properties. Cell Adh Migr. 2024;18:1-11. doi: 10.1080/19336918.2024.2316576. PubMed PMID: 38357988; PubMed Central PMCID: PMCPMC10878020.

8 Musi CA, Agro G, Santarella F, Iervasi E, Borsello T. JNK3 as Therapeutic Target and Biomarker in Neurodegenerative and Neurodevelopmental Brain Diseases. Cells. 2020;9. doi: 10.3390/cells9102190. PubMed PMID: 32998477; PubMed Central PMCID: PMCPMC7600688.

9 Bhowmick S, D'Mello V, Muneer PMA. Synergistic Inhibition of ERK1/2 and JNK, Not p38, Phosphorylation Ameliorates Neuronal Damages After Traumatic Brain Injury. Mol Neurobiol. 2019;56:1124-36. doi: 10.1007/s12035-018-1132-7. PubMed PMID: 29873042.

10 Jarrahi A, Braun M, Ahluwalia M, Gupta RV, Wilson M, Munie S, et al. Revisiting Traumatic Brain Injury: From Molecular Mechanisms to Therapeutic Interventions. Biomedicines. 2020;8. doi: 10.3390/biomedicines8100389. PubMed PMID: 33003373; PubMed Central PMCID: PMCPMC7601301.

11 Mehta J, Rolta R, Mehta BB, Kaushik N, Choi EH, Kaushik NK. Role of Dexamethasone and Methylprednisolone Corticosteroids in Coronavirus Disease 2019 Hospitalized Patients: A Review. Front Microbiol. 2022;13:813358. doi: 10.3389/fmicb.2022.813358. PubMed PMID: 35242118; PubMed Central PMCID: PMCPMC8886296.

12 Chen X, Zhang B, Chai Y, Dong B, Lei P, Jiang R, et al. Methylprednisolone exacerbates acute critical illness-related corticosteroid insufficiency associated with traumatic brain injury in rats. Brain Res. 2011;1382:298-307. doi: 10.1016/j.brainres.2011.01.045. PubMed PMID: 21262204.

13 Danielson M, Reinsfelt B, Westerlind A, Zetterberg H, Blennow K, Ricksten SE.

Effects of methylprednisolone on blood-brain barrier and cerebral inflammation in cardiac surgery-a randomized trial. J Neuroinflammation. 2018;15:283. doi: 10.1186/s12974-018-1318-y. PubMed PMID: 30261896; PubMed Central PMCID: PMCPMC6158839.

14 Yulug B, Kilic E, Altunay S, Ersavas C, Orhan C, Dalay A, et al. Cinnamon Polyphenol Extract Exerts Neuroprotective Activity in Traumatic Brain Injury in Male Mice. CNS Neurol Disord Drug Targets. 2018;17:439-47. doi: 10.2174/1871527317666180501110918. PubMed PMID: 29714150.

15 Khaksari M, Shahryari M, Raji-Amirhasani A, Soltani Z, Bibak B, Keshavarzi Z, et al. Aloe vera Leaf Extract Reduced BBB Permeability and Improved Neurological Results after Traumatic Brain Injury: The Role of Oxidative Stress. Oxid Med Cell Longev. 2024;2024:5586814. doi: 10.1155/2024/5586814. PubMed PMID: 39040520; PubMed Central PMCID: PMCPMC11262876.

16 Puglisi C, Yao TL, Milne R, Möller M, Middleton DJ. Generic recircumscription in the Loxocarpinae (Gesneriaceae), as inferred by phylogenetic and morphological data. TAXON. 2016;65:277-92. doi: 10.12705/652.5.

17 Purba EC, Silalahi M. The ethnomedicine of the Batak Karo people of Merdeka sub-district, North Sumatra, Indonesia. International Journal of Biological Research. 2016;4:181-9. doi: 10.14419/ijbr.v4i2.6493.

18 Ginting KB, Purwoko A, Simanjuntak J. Kearifan Lokal Dalam Pengelolaan Hutan di Desa Serdang Kecamatan Barusjahe, Kabupaten karo. Peronema Forestry Science Journal. 2015;4:186-99.

19 Bellavite P. Neuroprotective Potentials of Flavonoids: Experimental Studies and Mechanisms of Action. Antioxidants (Basel). 2023;12. doi: 10.3390/antiox12020280. PubMed PMID: 36829840; PubMed Central PMCID: PMCPMC9951959.

20 Ibrahim H, Uttu AJ, Sallau MS, Iyun ORA. Gas chromatography–mass spectrometry (GC–MS) analysis of ethyl acetate root bark extract of Strychnos innocua (Delile). Beni-Suef University Journal of Basic and Applied Sciences. 2021;10:65. doi: 10.1186/s43088-021-00156-1.

21 Khairani D, Ilyas S, Wati DP. Molecular Docking and Pharmacokinetic Evaluation of Nanoherbal Senduduk Bulu (Miconia Crenata (Vahl.) Michelang.) Compounds As AKT1 Inhibitors. Int J App Pharm. 2025;17:90-103. doi: 10.22159/ijap.2025v17i2.52932.

22 Padmi H, Kharisma VD, Ansori ANM, Sibero MT, Widyananda MH, Ullah ME, et al. Macroalgae bioactive compounds for the potential antiviral of SARS-CoV-2: An in silico study. J Pure Appl Microbiol. 2022;16:1018-27. doi: 10.22207/JPAM.16.2.26.

23 Wati DP, Ilyas S, Khairani D. In Silico Study of Compounds from Nanoherbal Jopan (Clibadium surinamense L.) Leaves as Inhibitors AKT1 Interaction. Trends in Sciences. 2024;22:8729. doi: 10.48048/tis.2024.8729.

24 Köhler T, Gutacker A, Mejía E. Industrial synthesis of reactive silicones: reaction mechanisms and processes. Organic Chemistry Frontiers. 2020;7:4108-20. doi: 10.1039/D0QO01075H.

25 Ferreri C, Masi A, Sansone A, Giacometti G, Larocca AV, Menounou G, et al. Fatty Acids in Membranes as Homeostatic, Metabolic and Nutritional Biomarkers: Recent Advancements in Analytics and Diagnostics. Diagnostics (Basel). 2016;7. doi: 10.3390/diagnostics7010001. PubMed PMID: 28025506; PubMed Central PMCID: PMCPMC5373010.

26 Santa-Maria C, Lopez-Enriquez S, Montserrat-de la Paz S, Geniz I, Reyes-Quiroz ME, Moreno M, et al. Update on Anti-Inflammatory Molecular Mechanisms Induced by Oleic Acid. Nutrients. 2023;15. doi: 10.3390/nu15010224. PubMed PMID: 36615882; PubMed Central PMCID: PMCPMC9824542.

27 Meng Q, Liu H, Wu H, Shun D, Tang C, Fu X, et al. A Network Pharmacology Study to Explore the Underlying Mechanism of Safflower (Carthamus tinctorius L.) in the Treatment of Coronary Heart Disease. Evid Based Complement Alternat Med. 2022;2022:3242015. doi: 10.1155/2022/3242015. PubMed PMID: 35607519; PubMed Central PMCID: PMCPMC9124127.

28 Hermanson GT. Chapter 13 - Silane Coupling Agents. In: Hermanson GT, editor. Bioconjugate Techniques (Second Edition). New York: Academic Press; 2008. p. 562-81. doi: 10.1016/B978-0-12-370501-3.00013-8.

29 Preeti, Sambhakar S, Saharan R, Narwal S, Malik R, Gahlot V, et al. Exploring LIPIDs for their potential to improves bioavailability of lipophilic drugs candidates: A review. Saudi Pharm J. 2023;31:101870. doi: 10.1016/j.jsps.2023.101870. PubMed PMID: 38053738; PubMed Central PMCID: PMCPMC10694332.

30 Seo Y, Lim H, Park H, Yu J, An J, Yoo HY, et al. Recent Progress of Lipid Nanoparticles-Based Lipophilic Drug Delivery: Focus on Surface Modifications. Pharmaceutics. 2023;15. doi: 10.3390/pharmaceutics15030772. PubMed PMID: 36986633; PubMed Central

PMCID: PMCPMC10058399.
31 Artursson P, Karlsson J. Correlation between oral drug absorption in humans and apparent drug permeability coefficients in human intestinal epithelial (Caco-2) cells. Biochem Biophys Res Commun. 1991;175:880-5. doi: 10.1016/0006-291x(91)91647-u. PubMed PMID: 1673839.
32 Gonzalez E, Jain S, Shah P, Torimoto-Katori N, Zakharov A, Nguyen Eth T, et al. Development of Robust Quantitative Structure-Activity Relationship Models for CYP2C9, CYP2D6, and CYP3A4 Catalysis and Inhibition. Drug Metab Dispos. 2021;49:822-32. doi: 10.1124/dmd.120.000320. PubMed PMID: 34183376; PubMed Central PMCID: PMCPMC11022912.
33 Magliocco G, Desmeules J, Matthey A, Quiros-Guerrero LM, Bararpour N, Joye T, et al. Metabolomics reveals biomarkers in human urine and plasma to predict cytochrome P450 2D6 (CYP2D6) activity. Br J Pharmacol. 2021;178:4708-25. doi: 10.1111/bph.15651. PubMed PMID: 34363609; PubMed Central PMCID: PMCPMC9290485.
34 Daina A, Zoete V. A BOILED-Egg To Predict Gastrointestinal Absorption and Brain Penetration of Small Molecules. ChemMedChem. 2016;11:1117-21. doi: 10.1002/cmdc.201600182. PubMed PMID: 27218427; PubMed Central PMCID: PMCPMC5089604.
35 Nawafleh S, Qaswal AB, Suleiman A, Alali O, Zayed FM, Al-Adwan MAO, et al. GABA Receptors Can Depolarize the Neuronal Membrane Potential via Quantum Tunneling of Chloride Ions: A Quantum Mathematical Study. Cells. 2022;11. doi: 10.3390/cells11071145. PubMed PMID: 35406709; PubMed Central PMCID: PMCPMC8998136.
36 Bramlett HM, Dietrich WD. Long-Term Consequences of Traumatic Brain Injury: Current Status of Potential Mechanisms of Injury and Neurological Outcomes. J Neurotrauma. 2015;32:1834-48. doi: 10.1089/neu.2014.3352. PubMed PMID: 25158206; PubMed Central PMCID: PMCPMC4677116.
37 Freire MAM, Rocha GS, Bittencourt LO, Falcao D, Lima RR, Cavalcanti J. Cellular and Molecular Pathophysiology of Traumatic Brain Injury: What Have We Learned So Far? Biology (Basel). 2023;12. doi: 10.3390/biology12081139. PubMed PMID: 37627023; PubMed Central PMCID: PMCPMC10452099.
38 Sachdev KR, Lynch KJ, Barreto GE. Exploration of novel ligands to target C-C Motif Chemokine Receptor 2 (CCR2) as a promising pharmacological treatment against traumatic brain injury. Biomed Pharmacother. 2022;151:113155. doi: 10.1016/j.biopha.2022.113155. PubMed PMID: 35598371.
39 Fesharaki-Zadeh A. Oxidative Stress in Traumatic Brain Injury. Int J Mol Sci. 2022;23. doi: 10.3390/ijms232113000. PubMed PMID: 36361792; PubMed Central PMCID: PMCPMC9657447.
40 Liu MD, Luo P, Wang ZJ, Fei Z. Changes of serum Tau, GFAP, TNF-alpha and malonaldehyde after blast-related traumatic brain injury. Chin J Traumatol. 2014;17:317-22. PubMed PMID: 25471424.